PERGAMON

Journal of Quantitative Spectroscopy & Radiative Transfer 83 (2004) 735–749

Journal of Quantitative Spectroscopy & Radiative Transfer

www.elsevier.com/locate/jqsrt

Absorption by water vapour in the 1 to 2 μm region

K.M. Smith[a,*], I. Ptashnik[b,c], D.A. Newnham[a], K.P. Shine[b]

[a] *Space Science and Technology Department, Rutherford Appleton Laboratory, Chilton Didcot, Oxfordshire OX11 OQX, UK*

[b] *Department of Meteorology, University of Reading, Reading, Berkshire RG6 6BB, UK*

[c] *Institute of Atmospheric Optics, Siberian Branch Russian Academy of Science, Russia*

Received 23 September 2002; received in revised form 28 January 2003; accepted 21 February 2003

Abstract

The near-IR (in the range 5000–10 000 cm^{-1}, 1–2 μm) bands of water vapour have been measured in absorption in the laboratory at sub-Doppler spectral resolution (up to 0.0054 cm^{-1} after numerical apodisation) by Fourier transform spectroscopy. Measurements have been made at 296 K on pure water vapour (at pressures between 2 and 20 hPa) and mixtures of water and air (at total pressures of 100 and 1000 hPa), at optical path lengths in the range 0.26–9.75 m. Measured absorption intensities have been compared with values calculated using the HITRAN 2000 molecular database. These comparisons indicate that the intensities of the $2v$(1.4 μm) and $2v+\delta$(1.14 μm) bands are underestimated in HITRAN 2000 by approximately 15% and 20%, respectively, for pure water vapour measurements, and 12% for both bands in the case of water–air mixtures. The $v+\delta$ (1.86 μm) band is in good agreement (0.4% for pure water vapour and less than 6% for mixtures with air) with HITRAN 2000. For typical atmospheric conditions, these absorption bands are sufficiently strong that radiation is fully absorbed at wavelengths in the region of the band centres. Hence the extra absorption that has been identified has only a modest impact (0.16 W m^{-2} or about 0.2%) on the global-mean clear-sky absorption of solar radiation. The impact in the upper troposphere is several times larger.

Keywords: Water vapour spectroscopy; Spectroscopic databases; Atmospheric absorption

1. Introduction

The interaction of the atmosphere with near-IR solar (short-wave) radiation is dominated by water vapour absorption. Understanding and characterising the amount and wavelength-dependence of absorption by water vapour and other atmospheric species is essential for climate studies. Model calculations of radiative transfer in the Earth's atmosphere rely on molecular spectral lines databases

* Corresponding author. Tel.: +44-1235-446475; fax: +44-1235-445848.
E-mail address: k.m.smith@rl.ac.uk (K.M. Smith).

0022-4073/04/$ - see front matter © 2003 Elsevier Ltd. All rights reserved.
doi:10.1016/S0022-4073(03)00119-5

such as HITRAN [1,2] to provide information about the spectral properties of molecules present in the atmosphere.

The state of our understanding of clear-sky absorption of solar radiation remains somewhat controversial. For example Wild and Ohmura [3], using broadband measurements of solar radiation, estimate that climate model radiation schemes underestimate absorption by 10%. Halthore and Schwartz [4] estimate a discrepancy of 4% at the atmospheric radiation measurement (ARM) Southern Great Plains site based on direct and diffuse broadband measurements. Brown et al. [5] and Mlawer et al. [6], using high and moderate resolution measurements in the spectral ranges 2000–10 000 cm^{-1} and 10 000–28 000 cm^{-1}, respectively, detected no anomaly. Given these conflicting results, it appears important to assess potential sources of the discrepancy through quantitative high-resolution spectroscopy of water vapour under well controlled and characterized conditions in the laboratory.

Our knowledge of water vapour line intensities has been receiving close scrutiny, and it has been suggested that atmospheric absorption by weak absorption lines absent from databases is important [7]. Also significant errors in database intensities for the stronger water vapour lines in the region 10 000–15 000 cm^{-1} (667 nm to 1 μm) have been found [8–10] to account for a small but nevertheless important fraction of the "missing" modelled absorption.

As part of a study into the role of water vapour in the Earth's climate, we report here a comparison of new laboratory measurements with data from HITRAN 2000 in the 5000–10 000 cm^{-1} (1–2 μm) spectral region. The HITRAN 2000 line intensity data for water vapour within this spectral region are derived from a combination of data carried over from the 1986 edition [11] and studies by Mandin et al. [12]. The final data from the study by Toth [13] so far have not been included in HITRAN and only unpublished data from the preliminary measurements have been included [14]. About 35% [14] of the total intensity in HITRAN 2000 for the region 5750–7965 cm^{-1} can be attributed to Toth's preliminary measurements, with the remainder originating from earlier studies [11]. Some of the original HITRAN data derived from the Mandin et al. [12] measurements have been corrected by Giver et al. [10].

Although a full line-by-line spectroscopic analysis of our new data has yet to be performed, the current study has already identified systematic errors in HITRAN water vapour line intensities within the range 6600–9200 cm^{-1} (1.09–1.52 μm).

2. Laboratory measurements

The near-infrared absorption spectra of pure water vapour and mixtures of water vapour with synthetic air have been characterised in the laboratory using the combination of a high-resolution Fourier transform spectrometer (FTS) and a short path-length absorption cell (SPAC) at the Rutherford Appleton Laboratory. The FTS was configured with a 150 W quartz tungsten halogen source, a calcium fluoride beam splitter, and a liquid nitrogen-cooled indium antimonide (InSb) detector. The SPAC, described in detail previously [15], was fitted with calcium fluoride windows for this work. The absorbing optical path within the SPAC was configured in one of two modes; gold coated White optics produced path lengths between 1.6 and 18.2 m in steps of 1.6 m, and a simpler double-pass arrangement with magnesium fluoride-coated aluminium mirrors gave continuously variable shorter path lengths in the range 19–86 cm. Good stability of the water vapour sample was achieved by

Table 1
Details of gas temperature, pressure, and humidity measurements with uncertainties

Measurement	Manufacturer and type	Stated uncertainty
Temperature		
Thermistors	RS Components *R–T* curve matched type UUA41J1	±0.2 K at 296 K
Signal logger	Laplace Instruments Model SPC-801	±0.3 K
Pressure		
0–10 hPa	MKS-390 (10 Torr Baratron)	±0.08% of reading
1–100 kPa	MKS-390 (1000 Torr Baratron)	±0.08% of reading
Atmospheric	Negretti aneroid barometer M2236A	±40 Pa
Humidity		
Relative humidity (RH)	Vaisala HMP234	
0–90% RH		±1%
90–100% RH		±2%
Temperature	Vaisala HMP234	±0.1 K

virtue of the small surface-area-to-volume ratio of the 19 cm internal diameter SPAC. For pure vapour samples the pressure typically varied by less than 10% over a 12 h measurement period.

High-resolution (between 0.0045 and 0.0068 cm^{-1} unapodised, where resolution is defined as 0.9/[maximum optical path difference in cm]) measurements of water vapour transmittance over optical path lengths of 29 cm and 4.9 m in the spectral region 5000–10 000 cm^{-1} (1–2 μm) were made. All of the measurements reported here were made at a gas cell temperature of approximately 296 K. Norton–Beer weak apodisation [16,17] and Mertz phase correction [18] were applied to all of the measured interferograms. The apodisation increases the width of spectral lines by a factor of 1.2 [16] compared to unapodised spectra. To reduce detected photon noise, optical filters were used to limit the optical bandwidth to the spectral range of the measurement. The interferometer aperture diameter was set such that the intensity of radiation at the detector was sufficient to give excellent information-to-noise ratios, whilst avoiding saturation of the detector or loss of spectral resolution. The alignment of the interferometer was optimised and the photometric accuracy tested before carrying out the measurements reported here. The FTS was maintained at a pressure below 0.4 Pa by a turbo-molecular pump to minimise the amount of carbon dioxide and water vapour in the optical path of the interferometer. A calcium fluoride window separates the FTS from the SPAC transfer optics. A rotary and turbo-molecular pump combination evacuated the transfer optics to a pressure below 0.02 Pa.

Details of the sensors used to measure gas temperature, pressure, and humidity within the SPAC are given in Table 1. The 10 and 1000 Torr full-scale Baratron (MKS, calibration traceable to NIST) pressure gauges were used during sample preparation and throughout the measurements. The atmospheric pressure reading of the 1000 Torr Baratron was compared with that of a calibrated (traceable to UK National Physical Laboratory standards) precision aneroid barometer. Low-pressure readings of the 10 and 1000 Torr Baratron gauges were compared by measuring identical pressures with both gauges. Relative humidity (RH) was measured with two humidity/PRT sensors positioned at opposite ends of the SPAC.

Water vapour samples were prepared from distilled liquid water (analar grade, BDH Chemicals) using a clean glass/PTFE vacuum line, and purified to remove dissolved air using at least three repeat 200 K freeze-pump-thaw cycles. Agreement between the humidity sensor and pressure gauge readings (to within the humidity sensor accuracy) confirmed the purity of the water vapour introduced to the SPAC. Purity-certified "zero" grade synthetic air (Air Products Ltd, 21% oxygen and 79% nitrogen) was added to water vapour in the SPAC to make mixtures at total pressures of either 100 or 1000 hPa. Despite the turbulent flow of the air into the SPAC, the humidity gauges indicated that at room temperature a stabilisation period of 1 h was required to achieve uniform mixing of the air with the water vapour. The total pressure, RH and temperature were recorded at 5 s intervals during spectroscopic measurements on water vapour samples. At least six spectroscopic measurements were made in each spectral region, for a range of water vapour partial pressures of between 2 and 20 hPa.

Evacuated-cell background spectra were recorded before and after each filling of the SPAC, at a spectral resolution of 0.03 cm^{-1}. Before each background spectrum was recorded, high-resolution test measurements were made to check that the water vapour had been adequately removed from the SPAC. The criterion for this was that the intensities of the strongest water vapour lines were reduced to the peak value of the spectral noise in the corresponding spectral region. Taking the ratio of the sample and averaged background spectra minimised errors in the transmittance or absorbance spectra from changes in baseline signal level, e.g. due to drifts in the near-IR source intensity. The r.m.s. signal-to-noise ratio in each of the transmittance spectra exceeded 1000:1 across the entire spectral range of the water vapour absorption features, giving an information-to-noise ratio in excess of 100:1 for all absorbances between 0.2 and 3.5, and a peak information-to-noise ratio of 370:1 for absorbances around 1.0.

3. Comparisons with the HITRAN 2000 database

The observed laboratory spectra were compared with Napierian absorbance spectra calculated for the measured laboratory conditions of temperature, pressure and humidity using HITRAN 2000 and the reference forward model (RFM) [19] line-by-line code. Detailed information about the optical configuration of the FTS and the numerical apodisation function was used to calculate a wavelength-dependent instrument line shape (ILS). This ideal ILS was convolved with the calculated molecular spectrum and the line shapes were found to match those observed in the laboratory measurements within the information-to-noise ratio of the spectra. Version 2.4 of the CKD [20] water vapour "continuum" model was included in the RFM/HITRAN calculations. This was implemented in conjunction with Voigt line shapes calculated to 25 cm^{-1} either side of line centre.

3.1. Measured and simulated spectra

The measured water vapour transmittance $\tau(\tilde{\nu}, T)$ at wave number $\tilde{\nu}$ (in cm^{-1}) and temperature T (in K) was calculated using

$$\tau(\tilde{\nu}, T) = \frac{I(\tilde{\nu}, T)}{I_0(\tilde{\nu}, T)}, \tag{1}$$

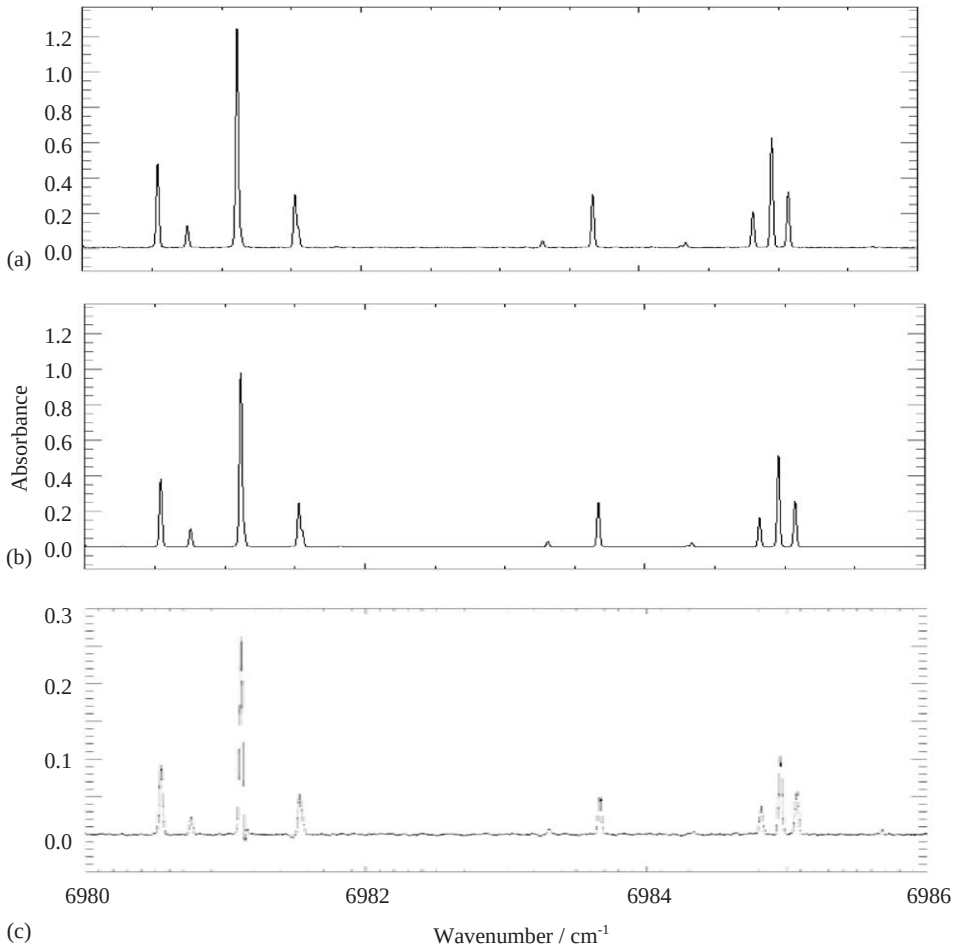

Fig. 1. Pure water vapour absorbance spectra at 296 K in the spectral region 6980–6986 cm^{-1}: (a) The measured absorbance for a sample of 2.2 hPa water vapour and a path length of 4.9 m at a spectral resolution of 0.0055 cm^{-1}; (b) the RFM/HITRAN 2000 calculated absorbance spectrum corresponding to the measurement; (c) the measured minus calculated residual absorbance spectrum.

where $I(\tilde{\nu}, T)$ and $I_0(\tilde{\nu}, T)$ are the intensities of the sample and background spectra, respectively. Absorbance spectra were calculated from the transmittance data using

$$A(\tilde{\nu}, T) = -\ln[\tau(\tilde{\nu}, T)]. \quad (2)$$

As an example, Figs. 1(a) and (b) show measured and calculated absorbance spectra for 2.2 hPa of pure water vapour at 296 K between 6980 and 6986 cm^{-1} over a path length of 4.9 m and at a spectral resolution of 0.0055 cm^{-1}. The difference between the measured and calculated absorbance is shown in Fig. 1(c). The residual spectrum shows that whilst the relative line positions and widths are in good agreement there is a substantial systematic difference in intensities. In this example, the absorbances of the measured lines exceed those of the RFM/HITRAN 2000 simulation by approximately 20%.

3.2. Intensity comparisons

Intensities of observed and calculated absorbance lines were compared by subdividing each absorption band into 1 or 2 cm^{-1} wide intervals. In each interval a Marquardt non-linear least-squares fit of the calculated spectrum to the observation was performed. For the pure water vapour measurements only those data where the calculated and observed Napierian absorbance was less than 1.0 were used in the comparisons to avoid introducing errors arising from saturation. In the case of the water vapour/air mixtures this absorbance threshold was relaxed to 3.5, since the air-broadened spectral lines were many times wider than the instrument resolution. The threshold of 3.5 was chosen because above this absorbance the information-to-noise ratio falls below 100:1. The state vector for the forward model in the fit included parameters that modelled the instrumental baseline (such as shifts due to instability of the near-IR source between sample and background measurements, or imperfect cancellation of optical filter channel fringes), a wave number calibration shift, and an absorbance scale factor. A fourth-order polynomial was used to model the instrumental baseline, and was adequate to fit the residual channel fringes within spectral intervals of 1 cm^{-1} within the range 5000–5800 cm^{-1} and 2 cm^{-1} within the ranges 6600–7600 cm^{-1} and 8400–9200 cm^{-1}. The instrumental baseline, wave number calibration shift and absorbance scaling factor were applied to the calculated spectrum such that the difference compared to the observation was minimised. In each interval the "best-fit" parameters were used to calculate a local baseline, and these were subtracted from the measured absorbance spectrum to correct for instrumental baseline effects. The integrated absorbance of the un-scaled calculated and baseline-corrected measured spectra were compared to determine mean integrated intensity ratios for each spectral interval. For each spectral interval, weighted-mean intensity ratios were calculated from at least three repeat measurements of water vapour at different concentrations and/or total pressures.

Separate calculations were carried out using data from the pure water vapour and water vapour–air measurements. The weighting factors were derived from the uncertainties arising from estimated errors in the measurement of water vapour concentration and uncertainties in the individual integrated intensity ratios. Within each 1–2 cm^{-1} wide spectral interval the integrated intensity ratios represent the scaling factors (SFs) that must be applied to HITRAN 2000 in order to obtain on average the same integrated absorption intensity as in observed spectra.

Figs. 2(a)–(c) show the weighted mean intensity SFs and associated errors for pure water vapour samples in the spectral regions 5000–5800 cm^{-1}, 6600–7600 cm^{-1} and 8400–9200 cm^{-1}, respectively. Figs. 3(a)–(c) show the corresponding factors and errors for water vapour–air mixtures in the same spectral regions. From Figs. 2(a)–(c) the SFs are approximately 1.00, 1.15 and 1.20, respectively. The results from the water vapour–air mixtures in Figs. 3(a)–(c) suggest slightly smaller SFs, but with larger error bars. The uncertainty in the water vapour concentration is larger for water–air mixtures than for pure vapour samples. This arises from the different methods used to determine water vapour concentration for pure vapour (measured using pressure gauges) and for mixtures of water vapour with air (measured using humidity sensors). However, without the humidity sensors, knowledge of the water vapour concentration the air mixtures would have been limited to the measured water vapour pressure before air was added. In this case it would have been necessary to make assumptions about the homogeneity of the mixture and the adsorption of water molecules onto the walls of the gas cell. In this respect the measurements on water–air mixtures reported here are a significant improvement on previous laboratory studies in this spectral region which appear to have

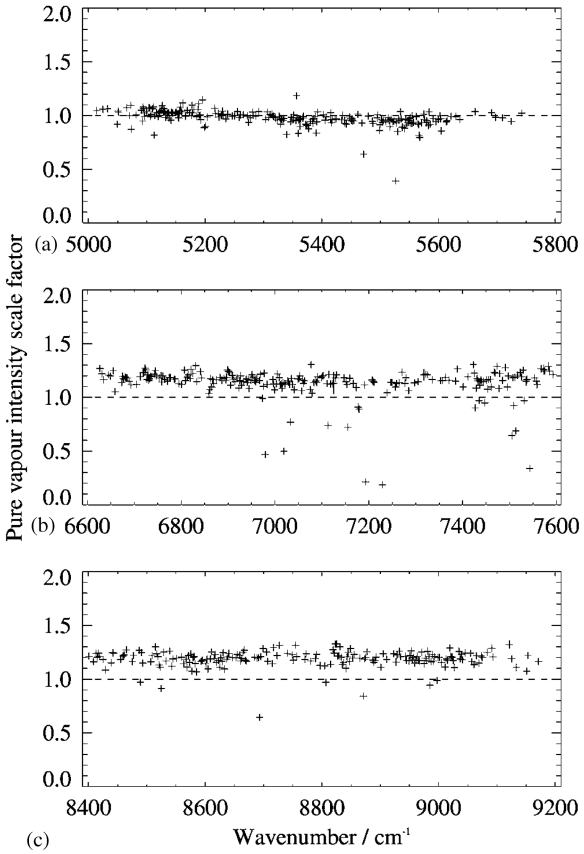

Fig. 2. HITRAN 2000 line intensity scaling factors derived from pure water vapour measurements at 296 K for (a) 5000–5800 cm^{-1}, (b) 6600–7600 cm^{-1} and (c) 8400–9200 cm^{-1}. Error bars indicate the known uncertainties in the scaling factors.

relied on knowledge of the water vapour pressure prior to mixing with air. The difference in the SFs derived from measurements on pure vapour and air mixtures is due to two main differences in their treatment. Firstly the maximum absorbance threshold used for the mixtures was higher than for pure vapour cases. Secondly for the water–air mixtures, pressure broadening redistributes absorbance away from the line centres and reduces peak absorbances. The combination of these two differences meant that some lines were excluded from the pure vapour intensity comparisons with HITRAN because they were too intense but these were included for the water–air mixture comparisons. Therefore the water–air SFs may give a better representation of systematic errors in HITRAN because they include more lines and lines with a larger range of intensities.

Where intensity SFs have been determined for both pure vapour and water–air mixtures a direct comparison can be made in corresponding spectral intervals, as shown in Figs. 4(a)–(c). In all three spectral regions most of the data lies below the dashed line, confirming that on average the scale factors determined from the water–air mixtures are smaller than those calculated using the pure vapour measurements. This discrepancy is most noticeable in Fig. 4(c).

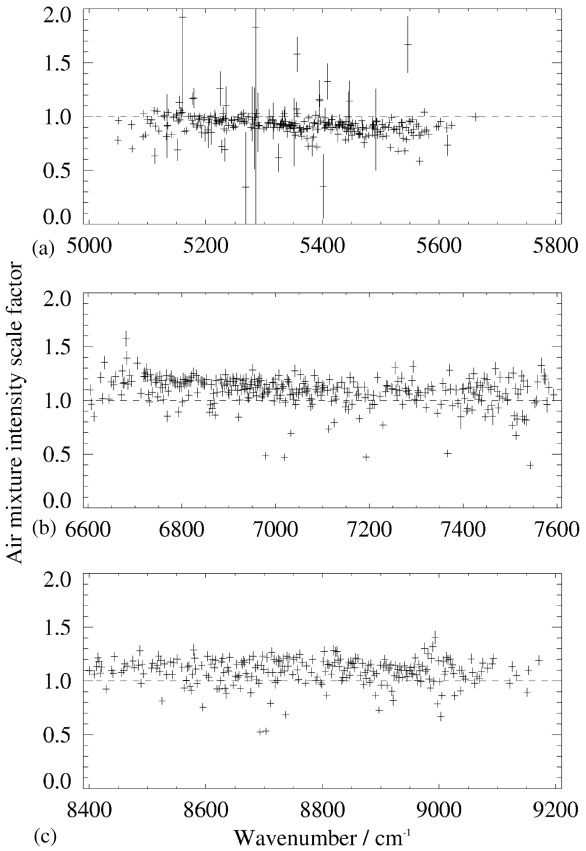

Fig. 3. HITRAN 2000 line intensity scaling factors derived from air-broadened water vapour measurements at 296 K for (a) 5000–5800 cm^{-1}, (b) 6600–7600 cm^{-1} and (c) 8400–9200 cm^{-1}. Error bars indicate the known uncertainties in the scaling factors.

Average SFs may be determined by comparing measured and calculated integrated absorbances for the entire spectral range of each band, excluding data in the spectral intervals where lines may be saturated. Mean SFs determined from individual measurements weighted by measurement uncertainties are given in Table 2. This method is not identical to calculating the mean of SFs from 1 or 2 cm^{-1} wide intervals across the whole band. The latter would lead to incorrect values for the average SF. Whilst these average SFs have limited use in high-resolution applications, they do provide an immediate indication of any systematic differences between the measurements and the database. The SFs in Table 2 are very similar to those shown in Figs. 2 and 3, which were derived from the smaller spectral intervals. The reasons for the differences between the SFs for the pure water vapour and water–air mixtures were discussed earlier.

We believe that the measurements described here represent an improvement on the data in HITRAN 2000 for this spectral region. Firstly, in those measurements covering the range 5750–7965 cm^{-1}, it was reported that there were "open spaces" reported in the optical path where additional water vapour in the laboratory air may have contributed to the absorption signal. Similarly, residual

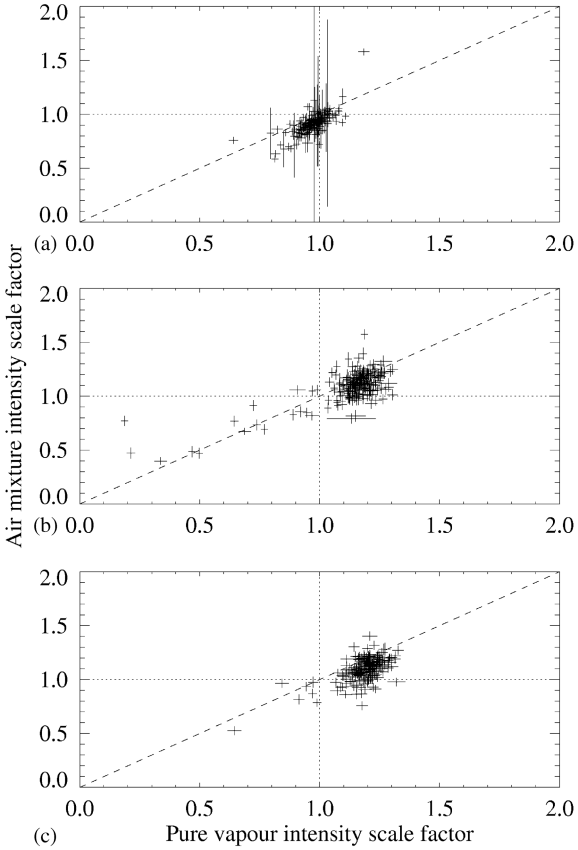

Fig. 4. A comparison of corresponding HITRAN 2000 intensity scaling factors derived from the pure water vapour and air-broadened water vapour measurements at 296 K for (a) 5000–5800 cm^{-1}, (b) 6600–7600 cm^{-1} and (c) 8400–9200 cm^{-1}. Error bars indicate the known uncertainties in both sets of scaling factors. In each spectral region the deviation of datapoints from the dashed line indicates disagreement between the two sets of scale factors, and deviation from the dotted lines indicates disagreement with HITRAN 2000 intensities.

water vapour in the spectrometer vacuum tank may have affected this and other earlier studies, if these contributions were not completely removed from the recorded spectra during post-measurement analyses. In our study we ensured that all optical paths outside of the absorption cell were evacuated to a pressure below 0.6 Pa, at which any residual water vapour has negligible absorbance compared to the water vapour sample in the gas cell (at most a pressure-path product of 9×10^{-3} m hPa). Furthermore, ratioing the sample spectra against empty cell background measurements should remove residual water vapour features arising from the spectrometer or transfer optics. Secondly, in the current study, measurements with pressure-path products as low as 0.58 m hPa were required to avoid degradation of the information-to-noise ratio due to spectral saturation of the strongest water vapour absorption lines. The smallest pressure-path product reported by Toth [13] of 3.4 m hPa was almost six times higher, and consequently intensities derived from these measurements were not included in HITRAN.

Table 2
Average intensity scaling factors for HITRAN 2000 water vapour absorption bands in the 1–2 μm region

Vibrational assignment	Wave number range/cm^{-1}	Wavelength range/μm	Pure water vapour scale factor	Water vapour/air mixture scale factor
$v+\delta$	5000–5800	1.72–2.00	0.996(2)	0.944(26)
$2v$	6600–7600	1.32–1.52	1.150(1)	1.120(48)
$2v+\delta$	8400–9200	1.09–1.19	1.204(19)	1.120(39)

The SFs are defined as the ratio of observed to calculated integrated absorbances and exclude spectral intervals containing lines that may be saturated. Standard deviations are given in parentheses.

It is interesting to note that in the region 5750–7965 cm^{-1} the line intensities derived from Toth's preliminary measurements are reported to be typically 25% smaller [14] than the preceding intensities included in the 1986 edition of HITRAN [11]. Furthermore, Toth's published intensities [13] are generally larger than the current HITRAN values that are based on his preliminary measurements, in some cases by up to 40% [14].

4. The impact on the absorption of solar radiation

To estimate the possible impact on the atmosphere of the extra water vapour absorption that we have identified using high resolution spectroscopy, solar irradiances reaching the surface were calculated and compared for the cases with and without SF corrections to HITRAN 2000. The air-broadened SFs were used because, despite their larger uncertainties compared to the SFs derived from measurements on pure water vapour, they were considered to be more representative of tropospheric conditions. The fast line-by-line code of Mitsel et al. [21] was used for high (0.001 cm^{-1}) spectral resolution calculation of optical depth for each of 17 atmospheric layers of clear-sky mid-season zonal-mean atmospheric profiles at a latitudinal resolution of 10°. The optical depth spectra were used then as input to the discrete ordinate (DISORT) code of Stamnes et al. [22] for irradiance calculations. Rayleigh scattering was taken into account using DISORT with four streams. Water vapour absorption is calculated using HITRAN 2000 with SF correction calculated in Section 3. The CKD 2.4 water vapour continuum is included. The solar irradiance at the top of atmosphere compiled by Kurucz [23] is employed, which represents the solar spectrum at a spectral resolution of 1 cm^{-1} (total solar irradiance = 1368.8 W m^{-2}).

Fig. 5a shows the downwelling solar irradiance at surface level for clear sky for a column water vapour amount of 25 kg m^{-2} and a solar zenith angle of 60°. Fig. 5b shows the extra absorption of irradiance (dF) due to the SF correction to HITRAN 2000. The dashed line in the upper plot is the cumulative additional absorption (i.e. the extra absorption integrated from 5000 cm^{-1} to the plotted wave number). As could be expected, the additional absorption is small (about 0.3 W m^{-2}), because of strong saturation of absorption between 7100 and 7400 cm^{-1}, with much of the extra absorption coming from the weaker (and hence less saturated) band near 8700 cm^{-1}.

In Fig. 6 the latitudinal dependence of extra absorption of solar irradiance due to the use of the SFs in the spectral region 5000–9200 cm^{-1} is presented for different seasons for clear-sky conditions. The global average value of extra absorption is 0.16 W m^{-2} or about 0.2% of the total clear-sky

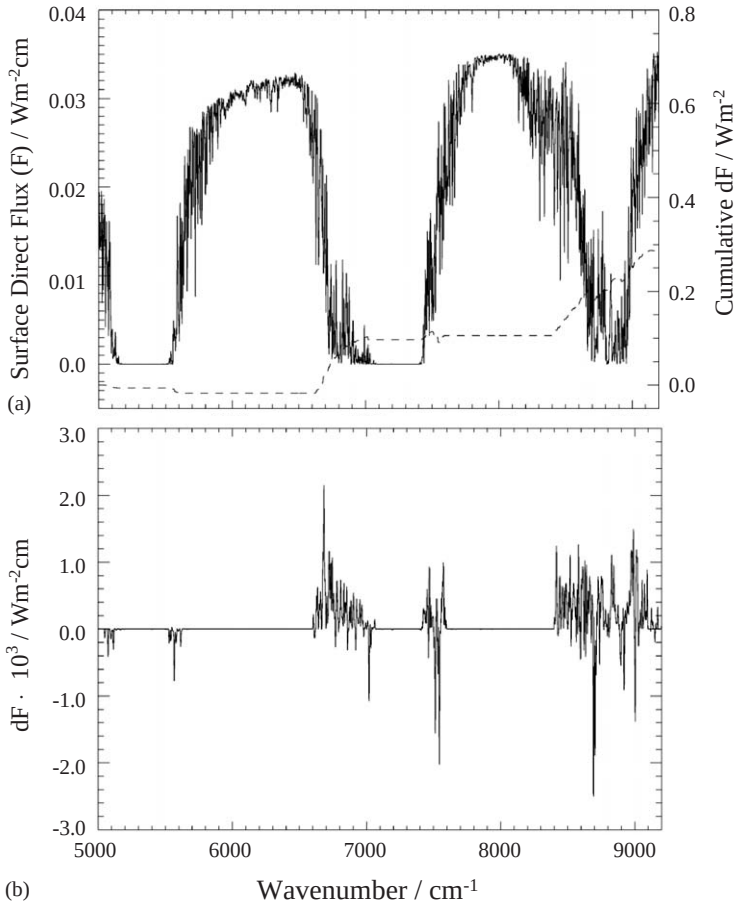

Fig. 5. The calculated solar direct flux at the surface (a) and the excess of absorbed irradiance (b) obtained from application of the scaling factors to HITRAN 2000 water vapour intensities in the spectral region 5000–9200 cm^{-1}. The dashed curve in (a) shows the cumulative value of extra absorption in W m^{-2} due to the use of the scaling factors. In this spectral region the integrated irradiance at surface level and the incident solar flux at the top of atmosphere are 72.5 and 135.43 Wm^{-2}, respectively. The water column was 25 kg m^{-2} and the solar zenith angle was 60°.

absorption. This is about an order of magnitude smaller than the impact of the corrections to the 0.82 and 0.94 μm bands derived in our earlier work [9]. The impact of the enhanced absorption is greatest at high-latitudes in summer time where the total water column is smaller; hence the absorption bands are less saturated than at lower latitudes and the impact of increases in absorption intensity is larger. This is in contrast to the impact of corrections to the weaker bands at wavelengths below 1 μm where the maximum impact is within 30° of the equator. The peak increase in Fig. 6, at the South Pole in January is about 0.5% of the total clear-sky absorption and is close to the impact of increased absorption by the shorter wavelength bands examined by Chagas et al. [9].

The influence of the saturation of these bands can be seen also in the Fig. 7, which shows the atmospheric heating rate due to water vapour absorption in the spectral region 5000–9200 cm^{-1} for a

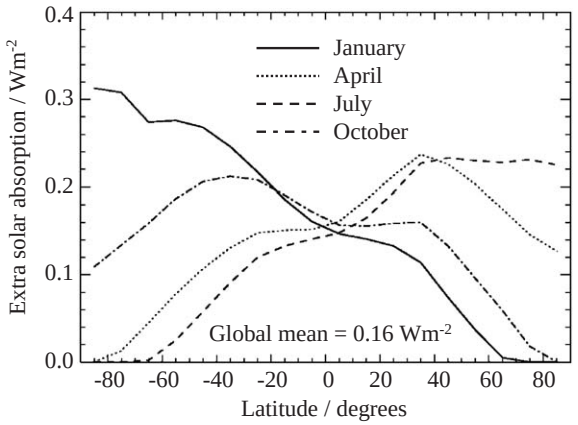

Fig. 6. The latitudinal and seasonal dependence of additional absorption of solar irradiance by water vapour from the intensity scaling factors applied to HITRAN 2000 in the spectral region 5000–9200 cm^{-1}. The global and annual mean value of the extra absorption is 0.16 W m^{-2}.

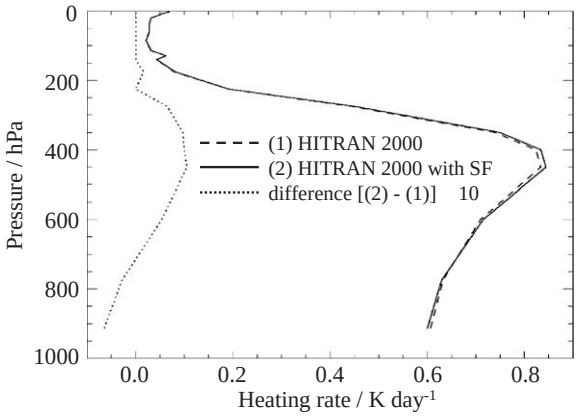

Fig. 7. The calculated atmospheric heating rate due to absorption of solar radiation by a 25 kg m^{-2} total column of water vapour in the spectral region 5000–9200 cm^{-1}, for a solar zenith angle of 60° and a surface albedo of 0.14. The solid and dashed curves represent the heating rates derived from HITRAN 2000 before and after application of the SF, respectively. The dotted curve shows the difference due to the scaling factors multiplied by a factor of 10.

globally averaged atmospheric profile and a solar zenith angle of 60°. The heating rate is enhanced because of the extra absorption in the upper troposphere by about 0.5%, with a corresponding decrease in heating rate in the lower troposphere.

Partridge and Schwenke [24] have made ab initio calculation of all rovibrational energy levels up to 40 000 cm^{-1}, line positions, and intensities for isotopic species of the water molecule. As a result the Partridge–Schwenke database contains about 127 500 water vapour lines in the spectral region 5000–9200 cm^{-1} compared to the 12 400 lines in HITRAN 2000. Although most of the additional lines are very weak their total effect can be significant in some cases.

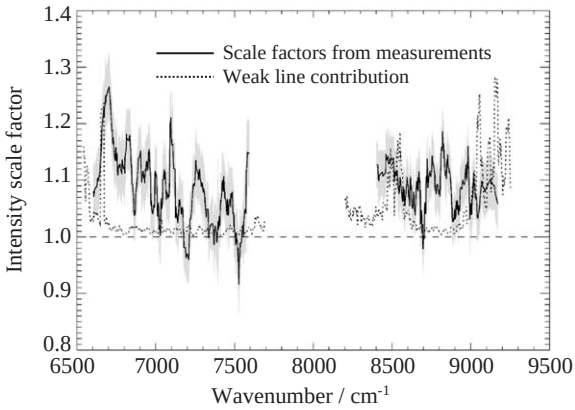

Fig. 8. The measured HITRAN SFs derived from the air-broadened measurements (solid curves) compared with those due to the weak lines proposed by Partridge and Schwenke [24] (dotted curves). Both sets of SFs are shown at a spectral resolution of 20 cm^{-1}. The grey shaded area represents the uncertainty on the SFs derived from the measurements.

In Fig. 8 the SFs derived from the combined air-broadened measurements are compared with SFs calculated from these additional weak lines. The set of the weak lines was obtained by subtracting the lines in HITRAN 2000 from the Partridge–Schwenke database. Lines in these two databases were compared by their quantum indexes. Our set of Partridge–Schwenke weak lines is in a good agreement with that derived independently by B.A. Fomin (personal communication).

It is apparent from Fig. 8 that the additional intensity from the lines proposed by Partridge and Schwenke [24] can generally only explain a small fraction of the SFs derived from our measurements. This implies that the main difference between our new measurements and HITRAN 2000 are largely due to the intensities in the lines already in the database, rather than missing absorption due to uncatalogued lines.

5. Conclusions

In the 5000–5800 cm^{-1} (1.72–2.0 μm) region the HITRAN 2000 database appears to provide a good representation of water vapour line intensities at 296 K, in pure vapour measurements and to a lesser extent in air-broadened spectra.

Our results for both the 6600–7600 cm^{-1} (1.32–1.52 μm) and the 8400–9200 cm^{-1} (1.09–1.19 μm) spectral regions show that substantial corrections are necessary to the HITRAN 2000 line intensities for both the cases of pure water vapour and water vapour–air mixtures. In the region 6600–7600 cm^{-1} the calculated pure vapour and water–air mixture line intensities are in error by approximately 15% and 12%, respectively. For some lines in this region discrepancies of up to 40% between HITRAN 2000 intensities and measurements by Toth [13] have already been identified by Giver et al. [14]. It is also interesting to note that despite the Giver et al. [10] corrections to the HITRAN database in the 8400–9200 cm^{-1} region there still appear to be significant systematic errors in line intensities of 20% and 12% for the pure vapour and air mixture cases, respectively.

Only a small proportion of these differences can be explained by the absence from HITRAN 2000 of the weak water vapour lines calculated by Partridge and Schwenke [24]. The strong saturation of absorption by water vapour in the atmosphere in the investigated spectral region (5000–9200 cm^{-1}, 1.09–2.0 μm) leads to a rather small extra absorption of solar radiation in spite of marked SF values for absorption bands near 7000 and 9000 cm^{-1} (1.42 and 1.11 μm). The global averaged value of extra clear-sky absorption is about 0.16 Wm^{-2} (or about 0.2% of the global mean). Although the revised line strengths may have limited importance for calculating the Earth's energy balance, they may be of much greater significance in other areas, such as remote sensing using these particular wavelength regions.

Acknowledgements

The authors thank the UK Natural Environment Research Council (for NERC grants NER/T/S/2000/00982 and NER/T/S/2000/01020 awarded to RAL and University of Reading respectively) and access to the Molecular Spectroscopy Facility at the Rutherford Appleton Laboratory. The technical assistance of R.G. Williams at the Rutherford Appleton Laboratory is acknowledged. We are grateful to Prof. B.A. Fomin for the fruitful discussions about the possible influence of the Partridge–Schwenke weak lines and providing us with his dataset for comparison. The authors also thank the reviewers for their very useful comments.

References

[1] Rothman LS, Rinsland CP, Goldman A, Massie ST, Edwards DP, Flaud J-M, Perrin A, Camy-Peyret C, Dana V, Mandin J-Y, Schroeder J, McCann A, Gamache RR, Wattson RB, Yoshino K, Chance KV, Jucks KW, Brown LR, Nemtchinov V, Varanasi P. The HITRAN Molecular Spectroscopic Database and Hawks (HITRAN Atmospheric Workstation): 1996 ed. J Quant Spectrosc Radiat Transfer 1998;60:665–710.

[2] Rothman LS, Chance K, Schroeder J, Goldman A. New Edition of HITRAN Database. Eleventh ARM Science Team Meeting Proceedings, Atlanta, Georgia, 2001.

[3] Wild M, Ohmura A. The role of clouds and the cloud-free atmosphere in the problem of underestimated absorption of solar radiation in GCM atmospheres. Phys Chem Earth B 1999;24:261–8.

[4] Halthore RN, Schwartz SE. Comparison of model-estimated and measured diffuse downward irradiance at surface in cloud-free skies. J Geophys Res 2000;105:20,165–77.

[5] Brown PD, Mlawer EJ, Clough SA, Shippert TR, Murcray FJ, Dybdahl AW, Harrison LC, Kiedron PW, Michalsky JJ. High-resolution model/measurement validations of solar direct-beam flux. Proceedings of the Ninth ARM Science Team Meeting, Atmospheric Radiation Measurement Program, San Antonio, Texas, 1999.

[6] Mlawer EJ, Brown PD, Clough SA, Harrison LC, Michalsky JJ, Kiedron PW, Shippert T. Comparison of spectral direct and diffuse solar irradiance measurements and calculations for cloud-free conditions. Geophys Res Lett 2000;27:2653–6.

[7] Learner RCM, Zhong W, Haigh JD, Belmiloud D, Clarke J. The contribution of unknown weak water vapor lines to the absorption of solar radiation. Geophys Res Lett 1999;26:3609–12.

[8] Belmiloud D, Schermaul R, Smith KM, Zobov NF, Brault JW, Learner RCM, Newnham DA, Tennyson J. New studies of the visible and near-infrared absorption by water vapour and some problems with the HITRAN database. Geophys Res Lett 2000;27:3703–6.

[9] Chagas JCS, Newnham DA, Smith KM, Shine KP. Effects of improvements in near-infrared water vapour line intensities on short-wave atmospheric absorption. Geophys Res Lett 2001;28:2401–4.

[10] Giver LP, Chackerian Jr. C, Varanasi P. Visible and near-infrared $H_2^{16}O$ line intensity corrections for HITRAN-96. J Quant Spectrosc Radiat Transfer 2000;66:101–5.

[11] Rothman LS, Gamache RR, Goldman A, Brown LR, Toth RA, Pickett HM, Poynter RL, Flaud J-M, Camy-Peyret C, Barbe A, Husson N, Rinsland CP, Smith MAH. The HITRAN database: 1986 ed. Appl Opt 1987;26:4058–97.
[12] Mandin JY, Chevillard J-P, Flaud J-M, Camy-Peyret C. $H_2^{16}O$ line positions and intensities between 8000 and 9500 cm^{-1}; the second hexad of interacting vibrational states: $\{(050),(130),(031),(210),(111),(012)\}$. Can J Phys 1988;66:997–1011.
[13] Toth RA. Extensive measurements of $H_2^{16}O$ line frequencies and strengths: 5750–7965 cm^{-1}. Appl Opt 1994;33: 4851–67.
[14] Giver LP, Chackerian C, Schwenke DW, Freedman RS, DiRosa MD, Varanasi P, Sams RL. Water vapor line intensity corrections and rovibrational assignment updates of the shortwave HITRAN and GEISA databases. Proceedings of the Tenth ARM Science Meeting, Atmospheric Radiation Measurement Program, San Antonio, Texas, 2000.
[15] Remedios JJ. D. Philosophical thesis, Oxford University, 1990.
[16] Norton RH, Beer R. New apodizing functions for Fourier spectrometry. J Opt Soc Am 1976;66:259–64.
[17] Norton RH, Beer R. New apodizing functions for Fourier spectrometry—Erratum. J Opt Soc Am 1977;67:419.
[18] Mertz L. Auxillary computation for Fourier transform spectrometry. Infrared Phys 1967;7:17–23.
[19] Dudhia A. Reference forward model version 3: Software user's manual, European Space Technology Center (ESTEC) Document PO-MA-OXF-GS-0003, European Space Agency (ESA), Paris, France, 1997.
[20] Clough SA, Kneizys FX, Davies RW. Line shape and the water vapor continuum. Atmos Res 1989;23:229–41.
[21] Mitsel AA, Ptashnik IV, Firsov KM, Fomin A. Efficient technique for line-by-line calculating the transmittance of the absorbing atmosphere. Atmos Oceanic Opt 1995;8:847–50.
[22] Stamnes K, Tsay SC, Wiscombe W, Jayaweera K. A numerically stable algorithm for Discrete-Ordinate-Method transfer in multiply scattering and emitting layered media. Appl Opt 1988;27:2502–9.
[23] Kurucz RL. http://cfaku5.harvard.edu/sun/irradiance/irradiancebins.dat, 1998.
[24] Partridge H, Schwenke DW. The determination of an accurate isotope potential energy surface for water from extensive ab initio calculation and experimental data. J Chem Phys 1997;106:4618–39.